12. 05. 2007. Progress in nuclear magnetic resonance spectroscopy (Revised)

High-pressure ^{17}O-NMR studies on Some Aqueous Polyoxoions in Water

Edina Balogh
Department of Chemistry
Department of Geology,
University of California, Davis, CA 95616
ebalogh@ucdavis.edu

William H. Casey*
Department of Chemistry
Department of Geology,
University of California, Davis, CA 95616.
whcasey@ucdavis.edu

(Received: November 12th 2007)

Keywords: high pressure NMR, clusters, exchange reaction, mechanism

Table of contests

1. Introduction

2. High-Pressure ^{17}O-NMR and Reaction Kinetics

2.1. ^{17}O-NMR Line-Broadening Methods

2.1.1. Diamagnetic Complexes with a Paramagnetic Relaxation Agent

2.1.2. Paramagnetic Complexes

2.2. High-Pressure ^{17}O-NMR Experiments

3. Review of Some Existing Work

3.1. Monomeric Complexes

3.1.1. Octahedrally Coordinated Metal-Aquo Ions

3.2. Hydrolytic Dinuclear Clusters

3.3. Trinuclear Aqueous Clusters

3.3.1. $[M_3(\mu_3\text{-}X)(\eta\text{-}X)_3(H_2O)_9]^{4+}$ Trinuclear Clusters

3.3.2. Acetate-Bridged Trinuclear Clusters

3.4. Some Isopolyanions and Polyoxometallate Molecules

3.4.1. Lindqvist ions

3.4.2. Decametallate Anions Related to Lindqvist Ions

3.4.3. Polyoxocations-Al(III) Keggin Clusters

3.4.4. Fe(III)-Keplerate Clusters

4. Conclusions

Acknowledgement

1. Introduction

Environmental chemistry and geochemistry have not traditionally been molecular fields. However, the environmental problems that could be solved easily are now largely controlled. Work in these fields now entails molecular chemistry, including the fate of certain pollutants, such as the estrogen disruptors, the toxicities of new anthropogenic compounds and the safety of radioactive waste in a repository that contains weathering nuclear fuel rods. Even subjects such as the biodegradation rates of xenobiotic toxicants requires molecular science since enantiomers do not degrade equally.

For aqueous reactions, perhaps the most important class to understand are ligand exchanges where one constituent in the inner-coordination-sphere of a metal is replaced with another, since these precede and control the rates of so many other processes. Replacement of the water molecule by another ligand is usually described by the Eigen-Wilkins mechanism, which is a two-step process. The first step is rapid formation of an outer-sphere ion pair by electrostatic forces. This step is so fast that equilibrium can be assumed. The second, and slower, step is loss of a water molecule so that the incoming ligand has a place to coordinate [1]:

$$M(H_2O)_6^{x+} + L^{n-} \rightleftharpoons \left[M(H_2O)_6, L\right]^{(x-n)+} \rightarrow M(H_2O)_5 L^{(x-n)+} + H_2O \quad (1)$$

where x=2, 3.

Even such a complicated process as dissolution of a soil mineral reduces to a series of ligand-exchange reactions where bridging oxygens are replaced by other nonbridging molecules [2]. In aqueous solutions, the most common ligand is the bound water molecule. The rate at which these bound water molecules leave the inner-

coordination sphere of the metal is, arguably, the most significant parameter for reactions in water.

Windows to this interfacial chemistry are provided by nanometer-size aqueous clusters. Casey and Swaddle [3] have argued that ligand-substitution reactions should not differ fundamentally between small metal-(hydr)oxo clusters and mineral surfaces as long as there is some structural similarity. In any case, experiments on small clusters should be used to validate computational methods of estimating the reaction parameters and used to inform cases, such as mineral surfaces, where experiments are impossible. Recently, Wang *et al.* used this approach to establish a correlation between calculated <Al-OH_2> bond lengths and rates of solvent exchange on experimental clusters and mineral surfaces that extends across many orders of magnitude [4]. In addition, recently our group provided a similar correlation between bond lengths and rates of ligand substitution for Fe(III) complexes, using a 2-nm-size Keplerate molecule for the key experiments [5].

Central to all of this work are ^{17}O-NMR spectroscopic measurements of the rates at which bound water molecules exchange with water in bulk solution. This exchange defines the most fundamental time scale for aqueous reactions and the rates span ~20 orders of magnitude for simple divalent and trivalent metals. Water exchange rates range from reactions that take over 200 years (Ir(III)) to those which reach completion in nanoseconds [6].

Most metal ions of geochemical importance react in subsecond time scales and thus are labile in the kinetic point of view. For these labile ions, the rates of exchange are determined from ^{17}O NMR line-broadening methods [7], which we review below. For inert metals, like Rh(III), oxygen exchanges can be monitored directly as changes of the

^{17}O NMR peaks as a function of time [8, 9]. In these experiments, the compound is either isotopically enriched and then dissolved into isotopically normal water, or an isotopically normal molecule is dissolved in ^{17}O-enriched solution. In either case, changes in the peak heights give the exchange rate.

In this article we review ligand-exchange rates and mechanisms for monomer complexes that can be compared to a larger nanocluster. Our goal is to identify trends in reactivities that scale with size of the cluster and that might be important for computation studies. The review also focuses narrowly on those clusters for which high-pressure ^{17}O-NMR have yielded activation parameters, because this method is now standard for assigning mechanisms.

2. High-Pressure ^{17}O-NMR and Reaction Kinetics

2.1. ^{17}O-NMR Line-Broadening Methods

2.1.1. Diamagnetic Complexes with a Paramagnetic Relaxation Agent

Ligand-exchange reactions for the aqueous ions of interest to geochemists are usually fast and require special NMR techniques. The most familiar method is the dynamic ^{17}O-NMR line-broadening technique [7, 10] where the rates of transverse relaxation ($1/T_2 = \pi \cdot FWHM$) are related to the rates of chemical exchange, where *FWHM* is the full-width at half-maximum of the ^{17}O-NMR signal. Conceptually, measuring the rate parameter is simply a matter of measuring the width of the ^{17}O-NMR peak corresponding to the bound water in the complex.

Cases that come close to this simple concept are diamagnetic ions. The peak for bound waters are usually clear and the only important complexity arises from quadrupolar relaxation, which can obscure the signal from chemical exchange, and the

fact that peak positions for bound and bulk waters can overlap. In such cases, the ^{17}O-NMR resonance from bulk water is broadened beyond detection by adding $Mn^{2+}_{(aq)}$ to the experimental solution (Fig. 1). The $Mn^{2+}_{(aq)}$ ion is paramagnetic and also exchanges its bound water molecules with bulk solution very quickly. The peak for the bulk water disappears when $Mn^{2+}_{(aq)}$ is added to the solution, leaving only the peak corresponding to the bound water [10]. It has been shown also that $Mn^{2+}_{(aq)}$ has no effect on the bound water [11].

Once the bulk-water signal is eliminated, the $1/T_2$ values for the bound water are estimated for several temperatures by monitoring the ^{17}O peak width. As mentioned above, the net signal contains two contributions:

$$\frac{1}{T_2} = \frac{1}{\tau_m} + \frac{1}{T_{2,q}} \qquad (2)$$

where τ_m is the mean lifetime of a water molecule in the inner-coordination sphere of the complex and $\frac{1}{T_{2,q}}$ is the intrinsic quadrupolar relaxation rate. The τ_m parameter is equal to $1/k_{ex}$, where k_{ex} is the water exchange rate, the desired parameter. Quadrupolar relaxation arises from interactions between the nucleus and the electric-field gradient.

Quadrupolar relaxation and chemical exchange have opposite temperature dependencies, which allow their contributions to $1/T_2$ to be resolved from one another via a temperature series of line-width measurements. Quadrupolar relaxation of the ^{17}O magnetism becomes more effective at low temperatures when the solution is viscous and the rotational correlation time is long. Chemical exchanges become more important at elevated temperatures as the reactions are thermally activated. Usually, an Arrhenius-like relation is used to approximate the quadrupolar relaxation [10]:

$$\frac{1}{T_{2,q}} = W_{q,298}\, e^{\frac{E_q}{RT}}. \qquad (3)$$

as a function of temperature, where E_q and W_q are fitting parameters. The temperature dependence of k_{ex}, the first-order rate coefficient for exchange of water molecules from the inner-coordination sphere to the bulk solution, takes the form of the Eyring equation:

$$\frac{1}{\tau_m} = k_{ex} = \frac{k_b T}{h}\, e^{\frac{\Delta S^{\neq}}{R}}\, e^{\frac{-\Delta H^{\neq}}{R T}} \qquad (4)$$

where k_b is Boltzmann's constant and the exponential terms include the activation entropy ($\Delta S^{\neq}$) and activation enthalpy ($\Delta H^{\neq}$) for chemical exchange. The parameters *T*, *R*, and *h* are absolute temperature, the gas constant, and Planck's constant, respectively.

2.1.2 Paramagnetic Complexes

Waters bound to paramagnetic metal ions are more complicated than those bound to diamagnetic metals. Unlike the diamagnetic ions, the $1/T_2$ values for bound waters alone usually cannot be measured directly from ^{17}O-NMR line widths. Rather, the $1/T_2$ values of the bulk solution, not the bound waters, are measured by the Carr-Purcell-Meiboom-Gill spin-echo technique [12] and interpreted to yield k_{ex}. Although the $1/T_2$ values remain the fundamental parameters needed to estimate k_{ex}, often the rates of longitudinal relaxation ($1/T_1$) and the ^{17}O resonance frequency (ω) are also measured as key parameters in a typical experiment. These other parameters are measured because they allow a better fit between the equations and data, and hence a more accurate estimate for k_{ex}. The $1/T_1$, $1/T_2$ and ω parameters are measured as a function of temperature and included in a set of equations (below) to constrain the value of k_{ex}.

The key information is the broadening of the bulk-water ^{17}O peak due to interactions with the paramagnetic ion. Thus, measurements on the sample are compared to a reference solution that has no paramagnetic ion to affect the NMR properties. The values of the ^{17}O parameters for the reference sample are denoted as: $1/T_{1A}$, $1/T_{2A}$ and ω_A and the difference of these parameters (sample minus the reference) are called the reduced parameters. These vary with the concentration of the paramagnetic complex in the solution.

$$\frac{1}{T_{1r}} = \frac{1}{P_m}\left[\frac{1}{T_1} - \frac{1}{T_{1A}}\right] \qquad (5)$$

$$\frac{1}{T_{2r}} = \frac{1}{P_m}\left[\frac{1}{T_2} - \frac{1}{T_{2A}}\right] \qquad (6)$$

$$\Delta\omega_r = \frac{1}{P_m}(\omega - \omega_A) \quad (7)$$

where P_m is the molar fraction of bound waters in the experimental solution.

These reduced parameter are fitted to the Swift and Connick equations [7] to yield the corresponding parameters for the bound water.

$$\frac{1}{T_{1r}} = \frac{1}{T_{1m} + \tau_m} \qquad (8)$$

$$\frac{1}{T_{2r}} = \frac{1}{\tau_m}\frac{T_{2m}^{-2} + \tau_m^{-1}T_{2m}^{-1} + \Delta\omega_m^2}{(\tau_m^{-1} + T_{2m}^{-1})^2 + \Delta\omega_m^2} \qquad (9)$$

$$\Delta\omega_r = \frac{\Delta\omega_m}{(1 + \tau_m T_{2m}^{-1})^2 + \tau_m^2\Delta\omega_m^2} \qquad (10)$$

The $1/T_{1m}$, $1/T_{2m}$ parameters are the longitudinal- and transverse-relaxation rates of the bound water and $\Delta\omega_m$ is the chemical shift difference between bound and bulk water. One typically fits experimental data to these three equations to estimate k_{ex} in a rate study

and, in the rest of this section, we discuss how the various terms are constrained. Although the parameters and equations might seem complicated, their practical implementation is fairly direct in a nonlinear least-squares fitting program.

The difference in frequency due to the paramagnetic ion, $\Delta\omega_m$, is proportional to the hyperfine- or scalar-coupling constant, $A/\hbar$ (Eq. 11):

$$\Delta\omega_{\mathrm{m}} = \frac{g_L \mu_{\mathrm{B}} S(S+1) B}{3 k_{\mathrm{B}} T} \frac{A}{\hbar} \quad (11)$$

where g_L is the isotropic Landé g factor, μ_B is the Bohr magneton, B represents the applied magnetic field, S is the electron spin and k_B is, again, the Boltzmann constant.

The longitudinal and transverse relaxation rates of the bound waters can be expressed as the sum of separate and independent contributions:

$$\frac{1}{T_{im}} = \frac{1}{T_{iq}} + \frac{1}{T_{isc}} + \frac{1}{T_{idd}} \qquad i=1,2 \quad (12)$$

The different terms dominating the longitudinal and transverse relaxation rates are considered separately below.

The ^{17}O longitudinal relaxation rate, $1/T_1$, is dominated by dipole-dipole and quadrupolar relaxation. The quadrupolar interaction is affected by the electric field gradient that is fixed in the molecular framework. Therefore as the molecule tumbles, quadrupolar energy is modulated, and spin lattice relaxation can be induced. This quadrupolar contribution can be expressed as [13]:

$$\frac{1}{T_{1q}} = \frac{3\pi^2}{10} \frac{2I+3}{I^2(2I-1)} \chi^2 (1+\eta^2/3) \tau_{\mathrm{RO}} \qquad (13)$$

while the dipole-dipole relaxation is:

$$\frac{1}{T_{1\mathrm{dd}}} = \left[\frac{1}{15}\left(\frac{\mu_0}{4\pi}\right)^2 \frac{\hbar^2\gamma_\mathrm{I}^2\gamma_\mathrm{S}^2}{r_\mathrm{MO}^6} S(S+1)\right] \times \left[6\tau_{1dd} + 14\frac{\tau_{2\mathrm{dd}}}{1+\omega_\mathrm{S}^2\tau_{2dd}^2}\right] \qquad (14)$$

where:

$$\frac{1}{\tau_{idd}} = \frac{1}{\tau_\mathrm{m}} + \frac{1}{\tau_\mathrm{RO}} + \frac{1}{T_{ie}} \qquad i = 1\ ,\ 2 \qquad (15)$$

and γ_S is the electron and γ_I is the nuclear gyromagnetic ratio (γ_S = 1.76 × 10^{11} rad s^{-1} T^{-1}, and for ^{17}O γ_I = -3.626 × 10^7 rad s^{-1} T^{-1}), μ_0 is the permeability constant ($\mu_0/4\pi = 1\times 10^{-7}$), $\hbar$ is the Planck's constant divided by 2π, r_{MO} is the M-O distance (where M is the paramagnetic metal ion), I is the nuclear spin (I=5/2 for ^{17}O), χ is the quadrupolar coupling constant and η is an asymmetry parameter, where $\chi(1+\eta^2/3)^{1/2}$ = 7.58 MHz using the quadrupolar coupling constant for ^{17}O in acidified water [14]. The r_{MO} distance is commonly estimated from crystallographic measurements but could conceivably be measured using EXAFS or another scattering technique.

The rotational correlation time, τ_{RO}, exhibits an inverse exponential dependence on temperature:

$$\tau_\mathrm{RO} = \tau_\mathrm{RO}^{298} \exp\left\{\frac{E_\mathrm{R}}{R}\left(\frac{1}{T} - \frac{1}{298.15}\right)\right\} \qquad (16)$$

In contrast to longitudinal relaxation, the scalar-relaxation term, manifested as $1/T_{2,sc}$, dominates the transverse relaxation rate. Thus, the relaxation rate for the bound water can be approximated as:

$$\frac{1}{T_{2,m}} \cong \frac{1}{T_{2,sc}} \qquad (17)$$

and then estimated from the equations for scalar coupling:

$$\frac{1}{T_{2\mathrm{m}}} \cong \frac{1}{T_{2\mathrm{sc}}} = \frac{S(S+1)}{3}\left(\frac{A}{\hbar}\right)^2\left(\tau_{s1} + \frac{\tau_{s2}}{1+\tau_{s2}^2\omega_s^2}\right) \qquad \frac{1}{\tau_{\mathrm{is}}} = \frac{1}{\tau_{\mathrm{m}}} + \frac{1}{T_{\mathrm{ie}}} \tag{18}$$

Within Eq. 18, the longitudinal electronic relaxation term ($1/T_{1\mathrm{e}}$) dominates and exerts the largest influence over the transverse relaxation rate ($1/T_{2\mathrm{m}}$). Within this term, the most important contributions arise from zero-field splitting and spin rotation. Previous work has shown that the dipole-dipole interaction term has little effect on $1/T_{1\mathrm{e}}$ [15].

For the electron-spin relaxation rates, $1/T_{1\mathrm{e}}$ and $1/T_{2\mathrm{e}}$, one can employ the equations developed by McLachlan [16]:

$$\left(\frac{1}{T_{1\mathrm{e}}}\right) = \frac{32}{25}\Delta^2\left(\frac{\tau_{\mathrm{v}}}{1+\omega_{\mathrm{S}}^2\tau_{\mathrm{v}}^2} + \frac{4\tau_{\mathrm{v}}}{1+4\omega_{\mathrm{S}}^2\tau_{\mathrm{v}}^2}\right) \tag{19}$$

$$\left(\frac{1}{T_{2\mathrm{e}}}\right) = \frac{32}{50}\Delta^2\left[3\tau_v + \frac{5\tau_v}{1+\omega_{\mathrm{S}}^2\tau_{\mathrm{v}}^2} + \frac{2\tau_v}{1+4\omega_S^2\tau_v^2}\right] \tag{20}$$

$$\tau_{\mathrm{v}} = \tau_{\mathrm{v}}^{298}\exp\left\{\frac{E_{\mathrm{v}}}{R}\left(\frac{1}{T} - \frac{1}{298.15}\right)\right\} \tag{21}$$

where Δ^2 is the trace of the square of the transient zero-field-splitting (ZFS) tensor, τ_{v} is the correlation time for the modulation of the ZFS with the activation energy (E_{v}), and ω_{s} is the Larmor frequency of the electron spin. In addition, the inverse binding time (or exchange rate, k_{ex}) of the water molecules in the inner sphere is also assumed to obey the Eyring equation (Eq. 22), where $\Delta\mathrm{S}^{\neq}$ and $\Delta\mathrm{H}^{\neq}$ are the entropy and enthalpy of activation for the exchange, and k_{ex}^{298} is the exchange rate at 298.15 K. For estimating $\Delta\mathrm{H}^{\neq}$, a convenient form is:

$$\frac{1}{\tau_{\mathrm{m}}} = k_{\mathrm{ex}} = \frac{k_{\mathrm{B}}T}{h}\exp\left\{\frac{\Delta S^{\neq}}{R} - \frac{\Delta H^{\neq}}{RT}\right\} = \frac{k_{\mathrm{ex}}^{298}T}{298.15}\exp\left\{\frac{\Delta H^{\neq}}{R}\left(\frac{1}{298.15} - \frac{1}{T}\right)\right\} \tag{22}$$

Eq. 22 is not a standard form of the Eyring equation but is particularly useful for isolating and calculating the $\Delta H^{\neq}$ term. The terms in the pre-exponential part of this equation are relatively well constrained by the equations presented above that estimate k_{ex}^{298}.

2.2. High-Pressure ^{17}O-NMR Experiments

In the last few decades, designs for high-pressure NMR probes have become widely available so that experiments can be conducted over the pressure range 10-400 MPa without difficulty. Thus, mechanisms of water exchange are now largely inferred from values of the activation volume ($\Delta V_0^{\neq}$) [11]. The pressure dependence of ln(k_{ex}) is expressed as an activated process:

$$\ln\left(\frac{1}{\tau_m}\right) = \ln k_{ex} = \ln(k_{ex})_0^T - \frac{\Delta V_0^{\neq}}{RT}P + \frac{\Delta\beta^{\neq}}{2RT}P^2 \qquad (23)$$

where $\Delta V_0^{\neq}$ is the activation volume at 298 K and $(k_{ex})_0^T$ is the water exchange rate at ambient pressure and temperature T and P is the applied pressure. The compressibility factor, $\beta^{\neq}$, is usually negligible for aqueous solutions and one typically observes a linear relationship between pressure and water exchange rate. The temperature is commonly adjusted by circulating a fluid from an external temperature bath and is controlled using a built-in platinum resistor.

The essential approach is simple: the pressure dependence of the exchange rate coefficient is measured and this leads to the mechanism [17-21]. By 'mechanism' we mean the structure of the transition state during the ligand exchange and how extensively the incoming ligand is involved. For a reaction involving bond elongation or bond breaking in the transition state, pressure increases slow down the reaction and one observes a decrease of $1/T_{2r}$ with pressure, corresponding to a dissociative (**D**) or

dissociative interchange (**I_d**) mechanism. Reaction mechanisms range from purely associative (**A**) to purely dissociative (**D**), corresponding to a reaction that has increased (**A**, $\Delta V_0^{\neq} << 0$) or decreased (**D**, $\Delta V_0^{\neq} >> 0$) coordination number in the transition state [22-25]. The errors on $\Delta V_0^{\neq}$ are usually about ±1 cm^3 mol^{-1} or about 10% of the $\Delta V_0^{\neq}$ value.

Most solvent-exchange reactions have some intermediate character, (**I_a** or **I_d**), where the transition involves a concerted motion involving the outer- and inner-coordination-sphere waters and an intermediate state. Interpretation of these mechanisms can be complicated [26, 27] but the mechanisms are key for evaluating computer simulations [28-31]. These simulations are becoming particularly important in the Earth and environmental sciences where hydrolytic reactions are so important and the environments cannot be easily sampled [32]. Save for a handful of studies [21, 33], including those by our group [34], there are no activation volumes for molecules with hydroxyl bridges.

The use of high-pressure NMR methods to assign reaction mechanisms is a particularly important development because, previously, the mechanisms were inferred from parameters such as activation entropies. These entropies are estimated by temperature extrapolations and are often inaccurate.

3. Review of Some Example Studies

3.1. Monomeric Complexes

3.1.1. Octahedrally Coordinated Metal-Aquo Ions

As mentioned above, replacement of a water molecule from the first coordination sphere of a monomer ion by a bulk water molecule has been extensively studied [10, 18,

19, 28, 35, 36]. The rates range over 20 orders of magnitude. Here we focus on the metals that are of particular interest to Earth scientists, including: V^{x+} (x=2, 3, 4), Al^{3+}, Fe^{3+}, Mo^{2+}, Cr^{3+} , Ru^{2+}, Rh^{3+} and that have been assembled into larger clusters that have also been kinetically characterized. Thus, a review of their monomer reactivities is the obvious place to begin a general discussion of clusters. The k_{ex}^{298} values for these hexaaqua complexes are compiled in Table 1 along with the activation parameters, including the $\Delta V_0^{\neq}$ values.

The Group 5b and 6b metals are worth discussing in detail because they make so many larger clusters of the polyoxometalate class, such as the Lindqvist ions and Keggin molecules. The system of aqueous vanadium structures is very complex since they form a large number of monomeric and polymeric hydrolysis products depending on total metal concentration and pH [37, 38]. Understanding these polymerization and dissociation reactions in detail would considerably advance our understanding of hydrolytic processes in general, including those proceeding at mineral surfaces, so we review them here.

Merbach and co-workers conducted high-pressure ^{17}O NMR experiments on the $V(H_2O)_6^{2+}$ ion and report $\Delta V_0^{\neq}$ = -4.1 cm^3mol^{-1} [18]. This metal was the second example of $\mathbf{I_a}$ exchange on a divalent and octahedrally coordinated transition metal ion. Later, further evidence was found for the associative mechanism of ligand exchange by using the high-pressure stopped-flow technique, as they followed the complexation between SCN^- and $V(H_2O)_6^{2+}$ [39]. High-pressure ^{17}O-NMR measurements were also conducted on the pentaquaoxovanadium ion $[VO(H_2O)_5]^{2+}$ and $\Delta V_0^{\neq}$ was found to be small and positive (+1.9 cm^3 mol^{-1}) [40]. Normally, water-exchange mechanisms generally become

more dissociative as the charge of the metal increases. However, in this case although the oxidation number of the vanadium changes from +2 to +4, the activation volume decreases. The pentaquaoxovanadium ion, however, has a double-bonded oxygen with strong d-p π bonding that influences the pathways for water exchange.

It is difficult to extend the comparison of mechanisms and oxidation to deeper within the Group 5b and Group 6b metals because one cannot carry out studies with Nb(V) and Ta(V); they do not form aquo ions. These pentavalent states are the stable ones in water and the molecules form oxo-terminated clusters, not monomer ions. However, Vanni *et al.* studied ligand exchange on the chloride and bromide complexes of the Nb(V) and Ta(V) in CH_2Cl_2 or CH_3Cl by high pressure ^1H NMR [41]. The reaction is exchange of a Lewis base, such as dimethyloxide (Me_2O), and not a bound water:

$$MX_5L + L^* \rightleftarrows MX_5L^* + L \qquad (24)$$

where X=Cl, Br and L and L^* are Lewis bases. They found that the solvent had no effect on the rate of ligand exchange reaction when it was carried out in chloroform or dichloromethane, and concluded that the solvent effect is negligible because the exchange reaction involves uncharged reactants and transition states.

Because of the lanthanide contraction, one expects Nb(V) and Ta(V) to be nearly identical the coordination geometry of their complexes and in electronic structure. They differ primarily in the extra full shell of electrons in the ground states (Kr versus Xe) and the full shell of $4f^{14}$ electrons in the Ta(V) structure, which are relatively deep in the core and well away from the valence shell. Thus, the ionic radius of Nb(V) and Ta(V) are nearly identical. Not surprisingly, the activation volumes for exchange of the solvent in

the metal pentachlorodimethyloxide are also similar in value; for $NbCl_5 \cdot Me_2O$ $\Delta V_0^{\neq}$ = +28.7 cm^3 mol^{-1} and for $TaCl_5 \cdot Me_2O$ $\Delta V_0^{\neq}$ = +27.8 cm^3 mol^{-1}). As a further example, the activation volumes for the exchange at the corresponding thioethers are: $\Delta V_0^{\neq}$ = -12.1 cm^3 mol^{-1} for $NbBr_5 \cdot Me_2S$ and $\Delta V_0^{\neq}$ = -12.6 cm^3 mol^{-1} for $TaBr_5 \cdot Me_2S$.

Furthermore, changes in the inner-coordination sphere are important. As the diameter of the nonexchanging halide ligand increases ($Br^- > Cl^-$), the volume of the first coordination sphere expands and the $\Delta V_0^{\neq}$ value increases, indicating a more dissociative pathway. Thus, the $\Delta V_0^{\neq}$ value is larger in a bromide complex than a similar chloride complex ($\Delta V_0^{\neq}$ = +28.7 cm^3 mol^{-1} for $TaCl_5 \cdot Me_2O$ and +30.5 cm^3 mol^{-1} for $TaBr_5 \cdot Me_2O$). Most interesting is the changeover in mechanism with otherwise similar ligands. For example, Vanni *et al*. report high-pressure kinetic data for $TaCl_5 \cdot Me_2O$, $TaCl_5 \cdot Me_2S$, $TaCl_5 \cdot Me_2Se$ and $TaCl_5 \cdot Me_2Te$ [41]. The $\Delta V_0^{\neq}$ values decrease dramatically, from +28.7 cm^3 mol^{-1} for exchange of Me_2O to -19.8 cm^3 mol^{-1} for exchange of Me_2S. The data for exchange of Me_2Se ($\Delta V_0^{\neq}$ = -18.7 cm^3 mol^{-1}) and Me_2Te ($\Delta V_0^{\neq}$ = -10.7 cm^3 mol^{-1}) more closely resemble the value for dimethylsulfide. The initial variation in $\Delta V_0^{\neq}$ is enormous and indicates a clear difference in mechanism between the oxide- and chalcogenide-containing ligands.

Other monomer complexes also exhibit a change in water-exchange mechanism as the metal changes charge, as an increased charge on the metal increases the strength of the M-O bond. Water exchange occurs via a dissociative intermediate mechanism (**I_d**; $\Delta V_0^{\neq}$ = +3.8 cm^3 mol^{-1}) for $Fe(H_2O)_6^{2+}$ with the exchange rate of k_{ex}^{298} = 4.39×10^6 s^{-1})

[17]. The same reaction on the $Fe(H_2O)_6^{3+}$ is ~10^4 times slower ($k_{ex}^{298} = 1.6 \times 10^2\ s^{-1}$) and the mechanism is **I$_a$**, associative intermediate ($\Delta V_0^{\neq} = -5.4\ cm^3\ mol^{-1}$) [42]. Thus, the weaker M-O bond strength of the $[Fe(H_2O)_6]^{2+}$ ion leads to a faster rate and a positive activation volume, indicating a more dissociative pathway.

For the d-block elements, high ligand-field stabilization energy is associated with kinetic inertness, therefore low-spin complexes are generally more inert than the high-spin ones [3]. Indeed the low spin t_{2g}^6 hexaaqua ions $[Ru(H_2O)_6]^{2+}$ and $[Rh(H_2O)_6]^{3+}$ are dramatically more inert than the first row d-block metal ions, with water exchange rates of $k_{ex}^{298} = 1.8 \times 10^{-2}\ s^{-1}$ [43] and $2.2 \times 10^{-9}\ s^{-1}$ [19], respectively. The inertness can be explained by the fact that the filled t_{2g}^6 orbitals spread out between the ligands and therefore the approach of the seventh molecule is electrostatically disfavored. This, and the observation that the exchange reaction is independent of the nature of the entering ligand [44] would suggest a dissociative mechanism; however, high-pressure NMR measurement gave a small negative activation volume ($\Delta V_0^{\neq} = -0.4\ cm^3\ mol^{-1}$). The authors assigned an **I** mechanism. The relative reactivities of the $[Ru(H_2O)_6]^{2+}$ and $[Ru(H_2O)_6]^{3+}$ ions, and their mechanisms of exchange, reflect the same tendencies as $[Fe(H_2O)_6]^{2+}$ and $[Fe(H_2O)_6]^{3+}$; that is, the bond strengths become weaker with reduced metal charge. A similar argument applies to the isoelectronic $[Ru(H_2O)_6]^{2+}$ and $[Rh(H_2O)_6]^{3+}$ ions. The $[Ru(H_2O)_6]^{2+}$ ion is more reactive, and has a more associative pathway for exchange, than the $[Rh(H_2O)_6]^{3+}$ ion because the charge is reduced.

All water exchange processes involving trivalent transition metal ions have negative activation volumes and therefore their water exchange mechanisms have considerable associative character: $[V(H_2O)_6]^{3+}$ $\Delta V_0^{\neq} = -8.9\ cm^3\ mol^{-1}$ [36], $[Cr(H_2O)_6]^{3+}$

$\Delta V_0^{\neq}$ = -9.6 cm^3 mol^{-1} [45] and $[Fe(H_2O)_6]^{3+}$ $\Delta V_0^{\neq}$ = -5.4 cm^3 mol^{-1} [35]. Therefore it is interesting to mention that the $[Al(H_2O)_6]^{3+}$ has a dissociative mechanism with an activation volume of $\Delta V_0^{\neq}$ = +5.7 cm^3 mol^{-1}. However, this can be explained by the sterical hindrance around the much smaller ion (ionic radii are V^{3+} 78 pm, Cr^{3+} 75.5 pm, Fe^{3+} 69 pm and Al^{3+} 54 pm), which makes it extraordinarily difficult to increase the coordination number [46]. Expansion of the coordination sphere in the transition state to accept an additional water molecule into octahedral Al(III) would be difficult.

3.2 Hydrolytic Dinuclear Clusters

In spite of the considerable amount of kinetic information on dissociation and condensation of dinuclear complexes [47], there are surprisingly few data for elementary reactions such as water exchanges. Crimp *et al.* used ^{18}O labeling techniques to follow the water exchanges on the Cr(III) hydrolytic dimer ($[(H_2O)_4Cr(\mu\text{-}OH)_2Cr(H_2O)_4]^{4+}$ and $[(H_2O)_4Cr(\mu\text{-}OH)_2Cr(OH)(H_2O)_3]^{3+}$) (Fig. 2) [48]. Later Dljaca *et al.* repeated the same study on Rh(III) dimer using ^{17}O-NMR, which complemented an earlier study that employed ^{18}O labeling [33]. Broadly similar results were obtained, namely that three pathways can be distinguished. Two of these pathways correspond to the coordinated water molecules occupying *cis* and *trans* positions relative to the bridging μ-OH groups. A slow and a fast exchange were identified, however the authors did not assign these rates to the *cis* or *trans* water molecules.

The rates of water exchanges were found to show a linear dependence on the proton concentration, indicating that the water exchange involves both the fully protonated and the monodeprotonated dimer. The calculated values are compiled in Table 2.

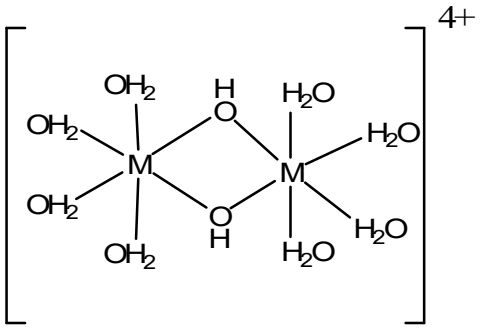

Figure 2. Structure of the hydrolytic dimer of $([(H_2O)_4M(\mu\text{-}OH)_2M(H_2O)_4]^{4+}$, where M=Cr(III) or Rh(III).

It is particularly interesting that a deprotonation of one water on these complexes does not affect the lability of the other. This point is important in light of data, presented below, concerning the lability of waters on trinuclear complexes.

Despite of the importance of high-pressure ^{17}O NMR measurements for determining the mechanism of the ligand exchange, only recently have researcher begun to examine the hydrolytic dimers. The first of these studies was performed on the hydroxo-bridged rhodium dimer, $[(H_2O)_4Rh(\mu\text{-}OH)_2Rh(H_2O)_4]^{4+}$ and the rates and mechanisms of the water exchange of the *cis* and *trans* water molecule were determined [21]. Exchange rates were found to be similar ($k_{trans}^{298} = 8.5 \times 10^{-7}$ s^{-1} and $k_{cis}^{298} = 5.4 \times 10^{-7}$ s^{-1}). For both type of oxygens highly positive activation volume values ($\Delta V_{0\ \mathrm{trans}}^{\neq} = 8.5$ cm^3 mol^{-1}and $\Delta V_{0\ \mathrm{cis}}^{\neq} = 10.1$ cm^3 mol^{-1}) were found, indicating an associative mechanism.

Sets of heteronuclear dinuclear complexes have been synthesized [49] that are isostructural with the Cr(III) and Rh(III) molecules. ^{17}O-NMR studies of the kinetics of water exchanges on these molecules could advance the field, particularly if the results are coupled to computation. To what extent, for example, are local bonding forces alone

responsible for the rates of substitution, or do the waters exhibit an averaged lability that reflects both metals in the complex?

3.3. Trinuclear Aqueous Clusters

There are two particularly interesting classes of trinuclear complexes that have at least one terminal water molecule per metal ion. For these two classes of clusters enough kinetic data exist to make general statements about reactivity trends. In the first class, sets of bound waters, which differ only in their positions relative to the central atom, exhibit profoundly different reactivities. The different reactivities of these waters present a profound challenge to computational chemists because, as we show, the cause of this difference in labilities remains unknown.

3.3.1 $[M_3(\mu_3\text{-}X)(\eta\text{-}X)_3(H_2O)_9]^{4+}$ Trinuclear Clusters

Since 1966, when Souchay *et al.* [50] first isolated the aqua ion of the molybdenum, several incomplete cuboidal trinuclear metal clusters have been identified and characterized kinetically. These types of clusters have the general stoichiometry: $[M_3(\mu_3\text{-}X)(\eta\text{-}X)_3(H_2O)_9]^{4+}$ where X= S, O M= Mo, W, Nb. (Fig. 3)

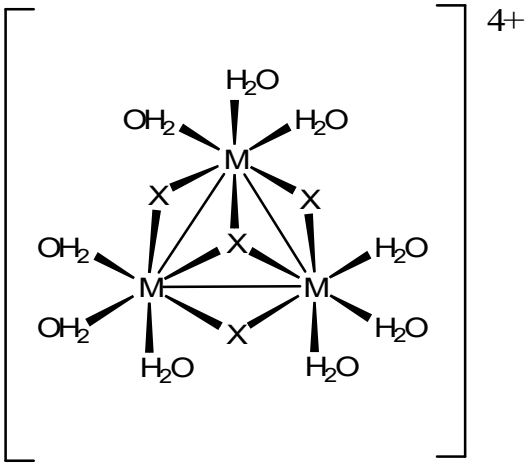

Figure 3. Stucture of $[M_3(\mu_3\text{-}X)(\eta\text{-}X)_3(H_2O)_9]^{4+}$ where X= S, O M= Mo, W, Nb.

The oxide- and sulfide-bridged versions provide a particularly interesting comparison. Richens *et al*. conducted ^{17}O NMR studies [51, 52] and the research group of Murmann showed with ^{18}O labeling [53] that the trinuclear unit (see Fig. 3) is retained in solution. Subsequently, numerous kinetic studies were carried out in order to determine the exchange rate of the terminal water molecules [52, 54-56]. The rates span an enormous range. Where the rates are particularly fast, kinetic parameters were determined by measuring transverse-relaxation times, as discussed above. For molecules with very slow reactions, the rate parameters were determined by isotopic injection followed by monitoring the peak intensities as a function of time.

A classic study was that of Richens et al. [52] who examined the $[Mo_3O_4(H_2O)_9]^{4+}$ trinuclear complex, which has four types of structural oxygens, all of which can be detected by ^{17}O NMR spectroscopy. The μ_2-O and central μ_3-O were found to be inert to exchange (labeled as "a" and "b", respectively in the original article, making "c" and "d" two types of bound waters), with a suspected half-life of several years. In addition to these inert bridging oxygens, the two sets of bound waters have distinct labilities. One molecule (labeled $^{c}H_2O$ in Table 3) lies *trans* to the μ_3-O and exchanges with an approximate rate ~10^5 slower than the other bound water ($^{d}H_2O$), which is in a position *trans* to the μ_2-O.

Water-exchange rates of the $^{c}H_2O$ were found to increase with increasing pH. Therefore, the exchange rate was described as:

$$k_{obs} = \frac{\left(k_{ex}\left[H^+\right] + K_a k_{OH}\right)}{\left[H^+\right] + K_a} \qquad (25)$$

However, in the fit, k_{ex} was found to be negligibly small and it was assumed that the rate coefficient for the fully protonated pathway could be ignored. Therefore, setting $k_{ex} = 0$, the reciprocal is:

$$\frac{1}{k_{obs}} = \frac{1}{k_{OH}} + \frac{1}{K_a \cdot k_{OH}}[H^+] \quad (26)$$

suggesting that the exchange occurs on the conjugate base involving a deprotonated $^{d}H_2O$, which is a bound hydroxyl.

The transverse relaxation rate is a sum of the contribution due to the exchange reaction and quadrupolar relaxation. The authors found that the transverse relaxation rate could be expressed as:

$$\frac{1}{T_{2obs}} = \frac{1}{T_{2q}} + \frac{K_a k_{OH}}{K_a + \left[H^+\right]} \quad (27)$$

The quadrupolar contribution is unaffected by changes in pH, which implies that the exchange rate depends on the proton concentration. In other words, the activation parameters for the bound hydroxyl (η-OH) can be expressed as:

$$k_{OH} = \frac{k_B T}{h}\left[\exp(\frac{\Delta S^{\neq}}{R} - \frac{\Delta H^{\neq}}{RT}\right] \quad (28)$$

From the positive value found for the activation entropy, the authors assigned a dissociative interchange mechanism to the reaction.

This study by Richens *et al.* [52] was remarkable because, besides being one of the earliest studies of water-exchanges from a trinuclear cluster, it raised fascinating questions about oxide labilities that remain unanswered to this day. In explaining the rapid exchange of the $^{d}H_2O$, the authors suggest that the ~10^5 difference in rates of exchange of the $^{c}H_2O$ and $^{d}H_2O$ resulted from partial formation of a bound hydroxyl

(^{d}OH), the conjugate base of the bound water. This bound hydroxyl is then assumed to exchange rapidly with the bulk solution and independently of the $^{c}H_2O$ site. One possible explanation for the Richens *et al.* result could be that deprotonation occurs via the formation of an intermolecular hydrogen bond. However, the X-ray crystal structures do not indicate such a $H_3O_2^-$ bridge.

It is unclear why the different oxygens exchange at such phenomenally different rates, but the reactivity trend even extends across to other metal systems. Of course, for octahedral metal aquo complexes, deprotonation of one of the bound waters is well known to labilize other bound waters, but in these cases the bound hydroxyl and bound waters interconvert rapidly by rapid proton exchange. In DFT calculations, the bond lengths between the metal and the bound hydroxyl are usually much shorter than bond lengths to bound waters, and are presumably stronger. Since bound hydroxyls are more tightly bonded to a metal site than a neutral water, one expects them to exchange more slowly. There are, however, no experimental studies of exchange of bound hydroxyls in structures where there is no doubt about the stoichiometry; that is, they are not undergoing rapid intercoversions with bound waters via proton exchange.

The reactivity trend is also robust. The molybdenum-oxide trinuclear complex can be synthesized with sulfurs in the bridging positions, giving a formula of $Mo_3S_4(H_2O)_9^{4+}$. As with the oxide molecule, there are two non-equivalent water molecules at the terminal positions. One water molecule per molybdenum is *trans* to the μ_3-S ($^{c}H_2O$) and two water molecules per molybdenum are *trans* to the μ_2-S ($^{d}H_2O$). Their reactivities follow the trend as found before for $Mo_3O_4(H_2O)_9$, namely that the $^{d}H_2O$ reacts ~10^5 faster than the $^{c}H_2O$. The increase of the $^{c}H_2O$ peak was followed as a

function of time, and was fitted to an exponential curve. The $^{d}H_2O$ peak was used as reference, as this, due to its much faster water exchange rate was already at isotopic equilibrium. Unlike the $[Mo_3O_4(H_2O)_9]^{4+}$, the signal of the $^{c}H_2O$ in the $[Mo_3S_4(H_2O)_9]^{4+}$ molecule does not exhibit a pH dependence in the pH range studied. The exchange rate was treated as mentioned above; that is, it was assumed that the $^{d}H_2O$ is fully deprotonated. From complex-formation experiments, an I_a mechanism was suggested [57].

A much higher lability for the $^{d}H_2O$ relative to the adjacent $^{c}H_2O$ was also found for on the $[Nb_3(\mu_3\text{-}Cl)(\eta\text{-}O)_3(H_2O)_9]^{4+}$ by Minhas *et al*. by ^{17}O NMR [58]. Thus this difference in the reactivities of these two bound waters, the $^{c}H_2O$ and $^{d}H_2O$, is a well-poised problem for simulation since there is some general chemistry manifested in similar molecules that transcends composition. Apparently, the difference in the reactivities of these two bound waters is a reflection of electronic effects that could be uncovered in simulation or simple steric crowding. It remains a tantalizing result.

3.3.2 Acetate-Bridged Trinuclear Clusters

The second class of trinuclear clusters are monooxo- or dioxo-capped acetate-bridged complexes, which have the general formula of $[M_3(\mu_3\text{-}O)_n(\eta\text{-}CH_3CO_2)_6(H_2O)_3]^{m+}$ M=Nb, Mo, W, n=1, 2, m=1, 2 [59-67]. Unlike the $[M_3(\mu_3\text{-}X)(\eta\text{-}X)_3(H_2O)_9]^{4+}$ clusters discussed above, these clusters have only one type of terminal water molecule. However, with these clusters, we can directly compare the effect of different bridging groups (acetate group, μ_2-O and μ_2-S) and metal ions on the reaction kinetics. Moreover, sets of clusters can be studied that differ in overall charge and that have a single oxo or a double-oxo cap in the center of the structure.

Powell *et al*. [68, 69] made the first kinetic studies on these ligands and determined water exchange rates (Table 3). They found that the $[Mo_3(\mu_3\text{-}O)_2(\eta\text{-}CH_3CO_2)_6(H_2O)_3]^{2+}$ and $[W_3(\mu_3\text{-}O)_2(\eta\text{-}CH_3CO_2)_6(H_2O)_3]^{2+}$ complexes have very similar exchange rates, though the tungsten version is slightly more inert than the molybdenum structure. This similarity in overall rates of exchange suggests that the activation enthalpies should also be similar [70], but this is not the case. The activation enthalpy for the tungsten molecule is slightly smaller than that of the molybdenum molecule, while the entropy is significantly negative.

These differences suggests that there is a changeover in the mechanism of solvent exchange when we replace the molybdenum with tungsten in these bioxo-capped clusters. Similar activation parameters were found for the monooxo capped $[W_3(\mu_3\text{-}O)(\eta\text{-}CH_3CO_2)_6(H_2O)_3]^{2+}$ although the rate constant is ~10^2 times larger. However, as we mentioned above, assignment of the reaction mechanism with indirect data, and activation entropies in particular, are often misleading.

In order to refine the assignments, high-pressure ^{17}O-NMR measurements were conducted on dioxo-capped acetato-bridged Mo(IV) and W(IV) trimers ($[M_3(\mu_3\text{-}O)_2(\eta\text{-}CH_3CO_2)_6(H_2O)_3]^{2+}$) [8]. The pressure dependence of the exchange rate confirmed this earlier suggestion for the mechanism. The activation volume of the Mo(IV) cluster is $\Delta V_0^{\neq}$ = + 8.0 (±0.4) cm^3mol^{-1}, leading to assignment of an associative mechanism, while for the isostructural W(IV) cluster $\Delta V_0^{\neq}$ = -1.9 (±0.2) $cm^3\ mol^{-1}$, consistent with an interchange mechanism with a dissociative character.

What is so remarkable about these two Mo(IV) and W(IV) clusters is that the $\Delta V_0^{\neq}$ values, and hence the mechanisms of reaction, are so profoundly different although

the molecules are structurally very similar to one another. The difference in $\Delta V_0^{\neq}$ for these isostructural molecules is the largest difference (~10 cm^3mol^{-1}) in activation volumes for any pair of *4d-5d* (and *3d-4d*) transition metal species located within the same group of the periodic table. These volumes exhibit a unique changeover in the water-exchange mechanism despite considerable similarities in molecular structure and reactivity. We will see below, in the section on Lindqvist ions, that the reactivities of other 4d-5d transition-metal clusters are also profoundly different even in cases where the structures are virtually identical and the molecules are nearly isoelectronic.

Water-exchange rate measurement on the mono oxo-capped ruthenium analogue of the trinuclear complexes mentioned above gave the first example of the correlation between the bond length and the exchange rate on metal complexes. Only 0.07 Å elongation on the M-O bond length (2.091 Å for $[Ru_3(\mu_3\text{-}O)(\eta\text{-}CH_3CO_2)_6(H_2O)_3]^+$ and 2.029 Å for $[Ru(H_2O)_6]^{3+}$ causes ~10^3 difference in exchange rate. Almost a decade later, a similar investigation was conducted on the $[Rh_3(\mu_3\text{-}O)(\eta\text{-}CH_3CO_2)_6(H_2O)_3]^+$ complex by Houston *et al*. [9]. The authors found that water exchange on the trimer occurs about ~10^4 times faster than on the dimer (5×10^{-3} s^{-1} *vs.* $k_{trans}^{298}= 8.5 \times 10^{-7}$ s^{-1} and $k_{cis}^{298}= 5.4 \times 10^{-7}$ s^{-1}) and about ~10^6 times faster than on the $[Rh(H_2O)_6]^{3+}$ (2.2×10^{-9} s^{-1}). The activation volume was found to be +5.3 cm^3 mol^{-1}.

3.4. Some Isopolyanions and Polyoxometallate Molecules

Here we discuss some systems that are well suited for high-pressure ^{17}O-NMR studies, although there is limited high-pressure NMR data to date on the clusters. The ^{17}O NMR method has proven to be extraordinarily useful for obtaining structural

information *in situ* for these molecules [71-74], and there have also been several pioneering kinetic studies [37, 75-81].

3.4.1. Lindqvist ions

The Lindqvist ions are one of the simplest classes of polyoxometalate anions (Fig. 4) and consist of a superoctahedron of six $M(O)_6$ octahedra that are linked by twelve μ_2-O(H) bridges at a μ_6-O. Each of the six Group 5b or 6b metals is terminated by a η=O. They have the stoichiometry: $[H_xM_6O_{19}]^{(8-x)-}$ where M=Nb(V), Ta(V) and $0 \leq x \leq 3$, and $[M_6O_{19}]^{2-}$ where M=Mo(VI), W(VI) and many varieties of substituted structures have been made [72, 82-87] including lacunary Lindqvist-like structures [71, 74, 88-98].

The Brønsted acidities of structural oxygens vary with the metal charges such that some molecules are so acidic (e.g., W(VI) and Mo(VI) ions) as to be unstable in water while others ([Nb(V) [Ta(V) ions) are unprotonated only at high pH conditions (pH>14). At lower-pH conditions, they form protonated species $[H_xM_6O_{19}]^{(8-x)-}$ where M=Nb(V), Ta(V) and $0 \leq x \leq 3$ and polymerize at pH<9.

The Nb(V) and Ta(V) Lindqvist ions are excellent kinetic models. They can be synthesized with ^{17}O in all sites and the constant ^{17}O-NMR signal from the inert μ_6-O indicates that they remain intact in solution while the structural oxygens isotopically equilibrate with solution. The $[H_xTa_6O_{19}]^{(8-x)-}$ and $[H_xNb_6O_{19}]^{(8-x)-}$ anions are also virtually isostructural (Table 4) due to the lanthanide contraction that essentially equalizes the <M-O> bond lengths. Overall reactivities of oxygen sites in the $[H_xTa_6O_{19}]^{(8-x)-}$ and $[H_xNb_6O_{19}]^{(8-x)-}$ ions are broadly similar, which is gratifying since they are nearly isostructural and isoelectronic, but differ profoundly in detail.

The relative reactivities of the η=O and μ_2-O(H) sites in the $[H_xTa_6O_{19}]^{(8-x)-}$ are opposite to those in the $[H_xNb_6O_{19}]^{(8-x)-}$ ion [99, 100]. For the $[H_xNb_6O_{19}]^{(8-x)-}$ ion in the pH range 12.5<pH<14.5, the rates of isotopic exchange of the η=O and μ_2-O(H) sites differ by about a factor of ten from one another, with the η=O sites reacting more slowly than the μ_2-O(H) sites. For the $[H_xTa_6O_{19}]^{(8-x)-}$ ion, the η=O site reacts about a factor of ten more rapidly than the μ_2-O(H) sites in the same pH region. For both molecules, the rates in the pH region of 12.5<pH<14.5 are largely independent of pH.

3.4.2 Decametallate Anions Related to Lindqvist Ions

Slightly more complicated are the decametallate ions of Group 5B metals, with most experiments conducted on the decavanadate $[V_{10}O_{28}]^{6-}$ [37, 76, 78] and, recently, the decaniobate $[Nb_{10}O_{28}]^{6-}$ ions [74]. The solid-state structures are well known [74, 101-105]. Although the decatantalate is suspected from ^{17}O-NMR data [74], it has not yet been crystallized or studied kinetically. These structures have seven structural oxygens and three distinct metal sites.

Several groups [76, 78] studied the oxygen exchange in the $[V_{10}O_{28}]^{6-}$ ion and find that the various structural oxygens in the decavanadate ion react at nearly identical rates, which points to an intermediate open structure. The rates increase at pH<4 and decrease at pH>6.3 and are approximately constant within these pH limits. Additionally, Murmann and Giese have reported $\Delta V_0^{\neq}$ = -5.0±2.0 cm^3 mol^{-1} for oxygen-isotope equilibration in all sites in the $[V_{10}O_{28}]^{6-}$ [37]. They used this value, and the fact that the oxygens react so similarly, to support their idea of a dissociation-mediated ^{18}O-exchange pathway. In their interpretation, the decavanadate partly dissociates into $[V_6O_{19}]^{8-}$ and $[V_4O_{11}]^{2-}$ bonded fragments that allow oxygen-isotope exchanges for all sites. As such,

their $\Delta V_0^{\neq}$ value includes the pressure dependence of the dissociation, which is presumably a metastable state, not a transition state.

Comba and Helm [78] extended and modified this interpretation. They employed ^{17}O- and ^{51}V-NMR to argue that the seven different oxygen sites actually differ in reactivity by a factor of ~2, which allowed them to speculate about the dissociation behavior. They suggested that dissociation of the decavanadate ion yields unstable $[V_6O_{19}]^{8-}$ and $[V_4O_{11}]^{2-}$ fragments. At the pH conditions of their investigation, (5<pH<5.5), these oligomers immediately undergo further dissociation to yield ring-like fragments $[(VO_3)_n]^{n-}$ (n=4, 5) that are stable and indeed observed in the study.

There are two key points from these studies. First, the structural oxygens in nanometer-size clusters exchange via complicated pathways that could not be uncovered by simulation alone. Secondly, there is much room for additional work on these molecules. A dimer of the decaniobate ion, having the approximate stoichiometry $[Nb_{20}O_{54}]^{8-}$, was recently discovered [106].

3.4.3. Polyoxocations-Al(III) Keggin Clusters

Data on aqueous clusters, such as the Al(III) Keggin clusters are immensely important to geochemists as experimental models that can yield kinetic data, particularly in light of recent work [107, 108] showing that such clusters are precursor to common iron- and aluminum-Earth materials. This most familiar class of Keggin-like molecules has the general formula of $[MO_4Al_{12}(OH)_{24}(H_2O)_{12}]^{7/8+}$ (Fig. 6), abbreviated as MAl_{12} where M=Al(III), Ga(III), Ge(IV) and they are structurally similar to the surface of Al-oxyhydoxide and clay minerals. Larger structures, including the 2-nm Al_{30} polyoxo cations $[Al_2O_8Al_{28}(OH)_{56}(H_2O)_{28}]^{18+}$ [109, 110] have been also synthesized.

The $GaAl_{12}$ version of the ε-Keggin cluster has been studied in some detail [34, 111]. These molecules have 24 bridging (μ_2-OH in two sets of twelve) and twelve terminal η-OH_2 oxygens, as well as four central μ_4-O that are kinetically inert to isotopic exchange. The two sets of μ_2-OH differ in reactivity considerably from one another. For the $GaAl_{12}$ molecules, the rates of exchange of the μ_2-OH^s (slow) and μ_2-OH^f (fast) sites differ by a factor of 44 (k_{ex}^{298} =677 h and 15.4 h respectively [112]). On the other hand, rates of water exchanges typically fall into the millisecond time scale at 298 K and are largely independent of the central metal (Table 5).

Loring *et al.* [34] conducted high-pressure ^{17}O-NMR experiments on the $GaAl_{12}$ molecule and reports $\Delta V_0^{\neq}$ values for oxygen-isotope exchanges at both the bound water and at one set of the hydroxyl bridges. Near 322 K, rates of exchange for the less labile set of bridging hydroxyls in the $GaAl_{12}$ decrease by factor of about two with increasing pressure from 0.1 to 350 MPa. These data indicate a substantially positive activation volume of $\Delta V_0^{\neq}$ = +7±1 cm^3mol^{-1}, which is the first activation volume measured for a bridging hydroxyl in a polynuclear complex. This result suggests significant bond-lengthening in the activation step. Electrostriction effects should be small because exchange occurs via a pH-independent path under the experimental conditions.

They also showed that the ^{17}O NMR linewidths for bound waters on the $GaAl_{12}$ complex decreases from 0.1 to 350 MPa, yielding an activation volume of $\Delta V_0^{\neq}$ = +2.8(±0.5) cm^3/mol. This activation volume is smaller than the value for the $[Al(H_2O)_6]^{3+}$ complex, suggesting that water exchange on the larger $GaAl_{12}$ complex has less dissociative character, although the average charge density is lower.

Computer simulations [113] showed that oxygen-isotope exchanges into the μ_2-OH are controlled by formation of a metastable open structure, as in the case of Lindqvist ions and $[V_{10}O_{28}]^{6-}$ decavanadate structures. In the MAl_{12} ε-Keggin cations, the extent to which the metastable structure forms is controlled by the strength of bonds between the central 'M' metal, which is tetrahedrally coordinated to the inert μ_4-O sites. Strong bonds here allow for facile formation of the metastable intermediate (and vice versa) by partial detachment of outer bonds, leading to rapid rates of oxygen isotope exchanges in the μ_2-OH. The rates of exchange of bound waters are unaffected by formation of the metastable intermediate, and are thus largely independent of the 'M' cation in the molecule composition, because the twelve water molecules exchange so much more rapidly than the μ_2-OH bridges.

The ^{17}O-NMR experiments on these MAl_{12} ε-Keggin polyoxocations re-emphasize conclusions stated above for the anion clusters. Pathways for exchanging bridging oxygens are complicated and largely proceed via metastable open structures. In the case of the MAl_{12} cations, this intermediate is a partly dissociated dimer-like moiety [111, 113]. In the case of the $[V_{10}O_{28}]^{6-}$ decavanadate ion, this open structure is purported to be bonded $[V_6O_{19}]^{8-}$ and $[V_4O_{11}]^{2-}$ fragments. In the case of the Nb(V) Lindqvist ion, the rates probably proceed via a metastable structure where one of the three mutually orthogonal $Nb_4(\mu_2\text{-}O)_4(\eta\text{-}O)_4$ rings partly opens and serves as a precursor to isotopic exchange. In all cases, the pathways are specific to the structure and non intuitive.

3.4.4. Fe(III)-Keplerate Clusters

Rates of ligand substitution onto the surfaces of Fe(III) and Al(III) colloids is a key question for Earth scientists. Rate of exchange of bound waters on the MAl_{12} ε-Keggin molecules are largely independent of small structural changes in the clusters, suggesting that these and similar clusters might be used as useful models for establishing general reactivity trends. With this in mind, our group conducted variable-temperature ^{17}O NMR experiments on the nanometer-sized Keplerate $Mo_{72}Fe_{30}$ cluster (Fig. 7), which contains on its surface 30 $Fe(H_2O)$ groups forming a well-defined icosidodecahedron [5]. This study showed that the rates of exchange of waters bound to the $>Fe^{III}\text{-}OH_2$ functional groups on this 2.5 nm molecule can be measured using standard ^{17}O-NMR methods.

The rates of water exchange from $>Fe^{III}\text{-}OH_2$ sites on the $Mo_{72}Fe_{30}$ complex are ~10^4 more rapid than for the simple aquo ion, $Fe(H_2O)_6^{3+}$, but slightly slower than for the Fe^{III}-EDTA and its derivatives (Table 6). Although data are sparse, and the coordination numbers differ among Fe(III) complexes in the table, the enhanced reactivity of these complexes correlates with a $<Fe^{III}\text{-}OH_2>$ bond length that is ~0.1 Å longer than in the $Fe(H_2O)_6^{3+}$ ion. This correlation resonates with other work. Recently, geochemists established a correlation between calculated $<Al\text{-}OH_2>$ bond lengths and rates of solvent exchange that extends across many orders of magnitude [4].

High-pressure ^{17}O-NMR experiments were also conducted, but we found that the cluster decomposed slightly under pressure, which precluded confident estimation of the $\Delta V_0^{\neq}$. It is clear, however, from increases in the reduced transverse relaxation time with pressure, along with the negative activation entropy, that the exchange mechanism has a dissociative character, such as a **D** or $\mathbf{I_d}$ mechanism. Although the number of

studies of large molecules is few, there is a strong correlation between bond lengths and rates of exchange.

4. Conclusions

Characterizing the reactive properties of nanometer-size aqueous clusters is the next big challenge for chemists and geochemists. Only via studies of these clusters, where the structures are known with great confidence, can reactivity be added to our understanding of structure. Key to this work will be high-pressure ^{17}O-NMR to determine $\Delta V_0^{\neq}$ values and thus water-exchange mechanism.

The ^{17}O-NMR studies to date indicate that bridges in oxide clusters react in complicated ways that challenge facile explanations derived from studies of aqueous monomer ions. The rates of isotopic exchange of some oxygen sites, such as the oxo sites in the Group VB polyoxoanions and μ_2-OH sites in the MAl_{12} series of aluminum polyoxocations, react via complicated structural intermediates. These intermediates are partly dissociated forms of the stable structures and are only inferred from kinetic data, and positive $\Delta V_0^{\neq}$ values in particular. On the other hand, rates of ligand substitution onto sites on Fe(III) and Al(III) clusters are robust and seem to scale with bond lengths, as one might expect. Correlations such as these could help Earth scientists enormously as new advances in methods of assigning structures to the aqueous interface are made.

These studies present clear challenges and test cases to computational chemists developing methods of simulating aqueous reactions. Particularly compelling data are available for the disparate rates of exchange of $^{c}H_2O$ and $^{d}H_2O$ on the trinuclear clusters, which differ by ~10^5, the profoundly different $\Delta V_0^{\neq}$ values for water exchanges on the tungsten and molybdenum trinuclear clusters, and the opposite reactivites of η=O and μ_2-

O(H) sites in the $[H_xTa_6O_{19}]^{(8-x)-}$ and $[H_xNb_6O_{19}]^{(8-x)-}$ Lindqvist ions. The future of aqueous chemistry and geochemistry lies in detailed study of these oxide clusters and largely via ^{17}O-NMR.

Acknowledgements

Support for this research was from the U.S. DOE via grant DE-FG03-02ER15325 and from the National Science Foundation (EAR 0515600). Thanks to Prof. Brian L. Phillips for help with Fig. 1.

5. References

[1] J. Burgess, Metal Ions in Solution, Ellis Horwood Limited, Chichester, (1978) 464.
[2] C. Ludwig, W. H. Casey, J. Colloid Interface Sci., 178 (1996) 176.
[3] W. H. Casey, T. W. Swaddle, Rev. Geophys., 41 (2003) 1.
[4] J. Wang, J. R. Rustad, W. H. Casey, Inorg. Chem., 46 (2007) 2962.
[5] E. Balogh, A. M. Todea, A. Müller, W. H. Casey, Inorg. Chem., 46 (2007) 7087.
[6] D. T. Richens, The chemistry of aqua ions. John Wiley, New York (1997) 592.
[7] T. J. Swift, R. E. Connick, J. Chem. Phys., 37 (1962) 307.
[8] J. R. Houston, D. T. Richens, W. H. Casey, Inorg. Chem., 45 (2006) 7962.
[9] J. R. Houston, P. Yu, W. H. Casey, Inorg. Chem., 44 (2005) 5176.
[10] D. Hugi-Cleary, L. Helm, A. E. Merbach, Helv. Chim. Acta, 68 (1985) 545.
[11] L. Helm, L. I. Elding, A. E. Merbach, Helv. Chim. Acta, 67 (1984) 1453.
[12] S. Meiboom, D. Gill, Rev. Sci. Instrum., 29 (1958) 688.
[13] R. K. Harris, Nuclear magnetic resonance spectroscopy: a physicochemical view. John Wiley (1983) 250.
[14] B. Halle, H. Wennerstroem, J. Chem. Phys., 75 (1981) 1928.
[15] D. H. Powell, O. M. Ni Dhubhghaill, D. Pubanz, L. Helm, Y. S. Lebedev, W. Schlaepfer, A. E. Merbach, J. Am. Chem. Soc., 118 (1996) 9333.
[16] A. D. McLachlan, Line widths of electron resonance spectra in solution. Proc. Roy. Soc. (London) Ser. A, 280 (1964) 271.
[17] Y. Ducommun, K. E. Newman, A. E. Merbach, Inorg. Chem., 18 (1980) 3696.
[18] Y. Ducommun, D. Zbinden, A. E. Merbach, Helv. Chim. Acta, 65 (1982) 1385.
[19] G. Laurenczy, I. Rapaport, D. Zbinden, A. E. Merbach, Magn. Reson. Chem., 29 (1991) S45.
[20] I. Dellavia, P. Y. Sauvageat, L. Helm, Y. Ducommun, A. E. Merbach, Inorg. Chem., 31 (1992) 792.
[21] A. Drljaca, A. Zahl, R. Van Eldik, Inorg. Chem., 37 (1998) 3948.
[22] C. H. Langford, H. B. Gray, Ligand Substitution Processes, W.A. Benjamin (1965) 160.
[23] A. E. Merbach, Pure Appl. Chem., 54 (1982) 1479.
[24] S. F. Lincoln, A. E. Merbach, Adv. Inorg. Chem., 42 (1995) 1.
[25] L. Helm, A. E. Merbach, Chem. Rev., 105 (2005) 1923.
[26] F. P. Rotzinger, Chem. Rev., 105 (2005) 2003.
[27] J. R. Rustad, A. G. Stack, J. Am. Chem. Soc., 128 (2006) 14778.
[28] T. Kowall, P. Caravan, H. Bourgeois, L. Helm, F. P. Rotzinger, A. E. Merbach, J. Am. Chem. Soc., 120 (1998) 6569.
[29] F. P. Rotzinger, J. Phys. Chem. A, 104 (2000) 8787.
[30] F. P. Rotzinger, J. Phys. Chem. A, 103 (1999) 9345.
[31] F. P. Rotzinger, J. Am. Chem. Soc., 119 (1997) 5230.
[32] W. H. Casey, J. R. Rustad, Annu. Rev. Earth Pl. Sci., 35 (2007) 21.
[33] A. Drljaca, L. Spiccia, H. R. Krouse, T. W. Swaddle, Inorg. Chem., 35 (1996) 985.
[34] J. Loring, P. Yu, B. L. Phillips, W. H. Casey, Geochim. Cosmochim Acta, 68 (2004) 2791.

[35] A. D. Hugi, L. Helm, A. E. Merbach, Helv. Chim. Acta, 68 (1985) 508.
[36] T. W. Swaddle, A. E. Merbach, Inorg. Chem., 20 (1981) 4212.
[37] R. K. Murmann, K. C. Giese, Inorg. Chem., 17 (1978) 1160.
[38] L. Pettersson, B. Hedman, I. Andersson, N. Ingri, Chem. Scripta, 22 (1983) 254.
[39] P. J. Nichols, Y. Ducommun, A. E. Merbach, Inorg. Chem., 22 (1983) 3993.
[40] Y. Kuroiwa, M. Harada, H. Tomiyasu, H. Fukutomi, Inorg. Chim. Acta, 146 (1988), 7.
[41] H. Vanni, A. E. Merbach, Inorg. Chem., 18 (1979) 2758.
[42] M. Grant, R. B. Jordan, Inorg. Chem., 20 (1981) 55.
[43] I. Rapaport, L. Helm, A. E. Merbach, P. Bernhard, A. Ludi, Inorg. Chem., 27 (1988) 873.
[44] N. Aebischer, G. Laurenczy, A. Ludi, A. E. Merbach, Inorg. Chem., 32 (1993) 2810.
[45] F. C. Xu, H. R. Krouse, T. W. Swaddle, Inorg. Chem., 24 (1985) 267.
[46] T. W. Swaddle, J. Rosenqvist, P. Yu, E. Bylaska, B. L. Phillips, W. H. Casey, Science, 308 (2005), 1450.
[47] J. Springborg, Adv. Inorg. Chem., 32 (1988) 55.
[48] S. J. Crimp, Stephen J.; L. Spiccia, H. R. Krouse, T. W. Swaddle, Inorg. Chem., 33 (1994) 465.
[49] S. J. Crimp, G. D. Fallon, L. Spiccia, Chem. Comm., 2 (1992) 197.
[50] P. Souchay, M. Cadiot, M. Duhameaux, Cr. Acad. Sci. C. Chim. 262 (1966) 1524.
[51] D. T. Richens, L. Helm, P. Pittet, A. E. Merbach, Inorg. Chim. Acta, 132 (1987) 85.
[52] D. T. Richens, L. Helm, P. Pittet, A. E. Merbach, F. Nicolo, G. Chapuis, Inorg. Chem, 28 (1989) 1394.
[53] K. R. Rodgers, K. R. Murmann, E. O. Schlemper, M. E. Shelton, Inorg. Chem., 24 (1985) 1313.
[54] B. L. Ooi, A. L. Petrou, A. G. Sykes, Inorg. Chem., 27 (1988) 3626.
[55] B. L. Ooi, A. G. Sykes, Inorg. Chem., 27 (1988) 310.
[56] B. L. Ooi, A. G. Sykes, Inorg. Chem., 28 (1989), 3799.
[57] D. T. Richens, P. A. Pittet, A. E. Merbach, M. Humanes, G. J. Lamprecht, B. L. Ooi, A. G. Sykes, Dalton Trans. Inorg. Chem., 15 (1993) 2305.
[58] S. Minhas, D. T. Richens, Dalton Trans. Inorg. Chem., 5 (1996) 703.
[59] A. Bino, F. A. Cotton, Z. Dori, S. Koch, H. Kueppers, M. Millar, J. C. Sekutowski, Inorg. Chem., 17 (1978) 3245.
[60] A. Bino, D. Gibson, Inorg. Chim. Acta, 65 (1982) 37.
[61] F. A. Cotton, Polyhedron, 5 (1986) 3.
[62] F. A. Cotton, M. P. Diebold, W. J. Roth, Inorg. Chem., 27 (1988) 3596.
[63] A. Bino, F.A. Cotton, Z. Dori, J. Am. Chem. Soc., 103 (1981) 243.
[64] A. Bino, F. A. Cotton, Z. Dori, M. Shaia-Gottlieb, M. Kapon, Inorg. Chem., 27 (1988) 3592.
[65] M. Ardon, A. Bino, F. A. Cotton, Z. Dori, M. Kaftory, G. Reisner, Inorg. Chem., 21 (1982) 1912.
[66] M. Ardon, A. Bino, F. A. Cotton, Z. Dori, B. W. S. Kolthammer, M. Kapon, Inorg. Chem., 20 (1981) 4083.
[67] M. Ardon, F. A. Cotton, Z. Dori, A. Fang, M. Kapon, G. M. Reisner, M. Shaia,

J. Am. Chem. Soc., 104 (1982) 5394.
[68] G. Powell, D. T. Richens, Inorg. Chem., 32 (1993) 4021.
[69] G. Powell, D. T. Richens, A. K. Powell, Inorg. Chim. Acta, 213 (1993) 147.
[70] D. Richens, Comments Inorg. Chem., 26 (2005) 217.
[71] M. Filowitz, W. G. Klemperer, L. Messerle, W. Shum, J. Am. Chem. Soc., 98 (1976) 2345.
[72] W. G. Klemperer, Angew. Chem., 90 (1978), 258.
[73] W. G. Klemperer, W. Shum, J. Am. Chem. Soc., 99 (1977) 3544.
[74] K. A. Marek, Personal Comm., (2001) 145
[75] O. W. Howarth, M. Jarrold, Dalton Trans. Inorg. Chem., 5 (1978) 503.
[76] R. K. Murmann, J. Am. Chem. Soc., 96 (1974) 7836.
[77] E. Heath, O.W. Howarth, Dalton Trans. Inorg. Chem., (1981) 1105.
[78] P. Comba, L. Helm, Helv. Chim. Acta, 71 (1988) 1406.
[79] C. L. Hill, Compr. Coord. Chem., 4 (2004) 679.
[80] A. T. Harrison, O. W. Howarth, Dalton Trans. Inorg. Chem., 9 (1985) 1953.
[81] A. T. Harrison, O. W. Howarth, Dalton Trans. Inorg. Chem., 6 (1985), 1173.
[82] C. J. Besecker, W. G. Klemperer, J. Am. Chem. Soc., 102 (1980) 7598.
[83] C. J. Besecker, W. G. Klemperer, V. W. Day, J. Am. Chem. Soc., 104 (1982) 6158.
[84] C. J. Besecker, V. W. Day, W. G. Klemperer, M. R. Thompson, J. Am. Chem. Soc., 106 (1984) 4125.
[85] C. J. Besecker, V. W. Day, W. G. Klemperer, Organometallics, 4 (1985), 564.
[86] V. W. Day, W. G. Klemperer, D. J. Maltbie, Organometallics, 4 (1985), 104.
[87] W. G. Klemperer, D. J. Main, Inorg. Chem., 29 (1990), 2355.
[88] A. D. English, J. P. Jesson, W. G. Klemperer, T. Mamouneas, L. Messerle, W. Shum, A. Tramontano, J. Am. Chem. Soc., 97 (1975) 4785.
[89] W. G. Klemperer, W. Shum, J. Am. Chem. Soc., 100 (1978) 4891.
[90] M. Filowitz, R. K. C. Ho, W. G. Klemperer, W. Shum, Inorg. Chem., 18 (1979) 93.
[91] W. G. Klemperer, NATO ASI Series, Series C: Mathematical and Physical Sciences, 103 (1983), 245.
[92] W. G. Klemperer, Inorg. Synth., 27 (1990) 71.
[93] T. M. Alam, M. Nyman, B. R. Cherry, J. M. Segall, L. E. Lybarger, J. Am. Chem. Soc., 126 (2004) 5610.
[94] M. Nyman, T. M. Alam, F. Bonhomme, M. A. Rodriguez, C. S. Frazer, M. E. Welk, J. Cluster Sci., 17 (2006) 197.
[95] M. Nyman, A. J. Celestian, J. B. Parise, G. P. Holland, T. M. Alam, Inorg. Chem., 45 (2006) 1043.
[96] R. P. Bontchev, M. Nyman, Angew. Chem., Int. Ed. 45 (2006), 6670.
[97] M. T. Pope, Compr. Coord. Chem. 4 (2004), 635.
[98] T. M. Anderson, M. A. Rodriguez, F. Bonhomme, J. N. Bixler, T. M. Alam, M. Nyman, Dalton Trans., 47 (2007) 4517.
[99] E. Balogh, T. M. Anderson, J. R. Rustad, M. Nyman, W. H. Casey, Inorg. Chem., 46 (2007) 7032.
[100] J. R. Black, M. Nyman, W. H. Casey, J. Am. Chem. Soc., 128 (2006), 14712.
[101] H. T. Evans, Inorg. Chem., 5 (1966) 967.

[102] H. T. Evans, A. G. Swallow, W. H. Barnes, J. Am. Chem. Soc., 86 (1964) 4209.
[103] A. G. Swallow, F. R. Ahmed, W. H. Barnes, Acts Cryst., 21 (1966) 397.
[104] E. J. Graeber, B. Morosin, Acta Crystall. B Stru., B33 (1977) 2137.
[105] V. W. Day, W. G. Klemperer, D. J. Maltbie, J. Am. Chem. Soc., 109 (1987), 2991.
[106] M. Maekawa, Y. Ozawa, A. Yagasaki, Inorg. Chem., 45 (2006) 9608.
[107] G. Furrer, B. L. Phillips, K-U. Ulrich, R. Pothig, W. H. Casey, Science, 297 (2002) 2245.
[108] F. M. Michel, L. Ehm, S. M. Antao, P. L. Lee, P. J. Chupas, G. Liu, D. R. Strongin, M. A. A. Schoonen, B. L. Phillip, J. B. Parise, Science, 316 (2007) 1726.
[109] L. Allouche, C. Gerardin, T. Loiseau, G. Ferey, F. Taulelle, Angew. Chem. Int. Ed., 39 (2000) 511.
[110] J. Rowsell, L.F. Nazar, J. Am. Chem. Soc., 122 (2000) 3777.
[111] W. H. Casey, Chem. Rev., 106 (2006) 1.
[112] W. H. Casey, B. L. Phillips, Geochim. Cosmochim. Acta, 65 (2001) 705.
[113] J. R. Rustad, J. S. Loring, W. H. Casey, Geochim. Cosmochim. Acta, 68 (2004) 3011.
[114] B. L. Phillips, S. N. Crawford, W.H. Casey, Geochim. Cosmochim. Acta, 61 (1997) 4965.
[115] F. Pickhard, H. Hartl, Z. Anorg. Allgem. Chem, 623 (1997) 1311.
[116] H. Hartl, F. Pickhard, F. Emmerling, C. Roehr, Z. Anorg. Allgem. Chem, 627 (2001) 2630.
[117] J. P. Nordin, D. J. Sullivan, B. L. Phillips, W. H. Casey, Geochim. Cosmochim. Acta, 63 (1999), 3513.
[118] P. Yu, B. L. Phillips, W. H. Casey, Inorg. Chem., 40 (2001) 4750.
[119] D. J. Sullivan, J. P. Nordin, B. L. Phillips, W. H. Casey, Geochim. Cosmochim. Acta, 63 (1999), 1471.
[120] W. H. Casey, B. L. Phillips, P. Nordin, D. J. Sullivan, Geochim. Cosmochim. Acta, 62 (1998) 2789.
[121] W. H. Casey, B. L. Phillips, M. Karlsson, S. Nordin, J. P. Nordin, D. J. Sullivan, S. Neugebauer-Crawford, Geochim. Cosmochim. Acta, 64 (2000) 2951.
[122] B. L. Phillips, W. H. Casey, M. Karisson, Nature, 404 (2000) 379.
[123] A. P. Lee, B. L. Phillips, W. H. Casey, Geochim. Cosmochim. Acta, 66 (2002) 577.
[124] B. L. Phillips, A. Lee, W. H. Casey, Geochim. Cosmochim. Acta, 67 (2003) 2725.
[125] T. Schneppensieper, S. Seibig, A. Zahl, P. Tregloan, R. van Eldik, Inorg. Chem., 40 (2001) 3670.

Table 1. Water exchange parameters obtained for different hexaqua complexes at 25°C

Complex	k_{ex}^{298} (s^{-1})	$\Delta S^{\neq}$ (J $mol^{-1}K^{-1}$)	$\Delta H^{\neq}$ (kJ mol^{-1})	$\Delta V_0^{\neq}$ (cm^3mol^{-1})	Reference
$[V(H_2O)_6]^{2+}$	8.7×10^1	-0.4	61.8	-4.1	[18]
$[V(H_2O)_6]^{3+}$	5.0×10^2	-28	49.4	-8.9	[36]
$[Al(H_2O)_6]^{3+}$	1.29	46.1	84.7	+5.7	[10]
$[Al(H_2O)_6]^{3+}$	2	-1.4	70		[114]
$[Cr(H_2O)_6]^{3+}$	2.4×10^{-6}	11	108	-9.6	[45]
$[Rh(H_2O)_6]^{3+}$	2.2×10^{-9}	29	131	-4.2	[19]
$[Ru(H_2O)_6]^{2+}$	1.8×10^{-2}	16.1	87.8	-0.4	[43]
$[Ru(H_2O)_6]^{3+}$	3.5×10^{-6}	-48.3	89.8	-8.3	[43]
$[Fe(H_2O)_6]^{3+}$	1.6×10^{2} [a]	2.9	15.3[a]	-5.4[b]	a. [42] b. [35]

Table 2. Water-exchange parameters at 25°C of Cr(III) and Rh(III) dinuclear clusters

Complex[§]		k_{ex}^{298} (s^{-1})	$\Delta S^{\neq}$ (J $mol^{-1}K^{-1}$)	$\Delta H^{\neq}$ (kJ mol^{-1})	Reference
Rh_2^{4+}	Fast	8.5×10^{-6}	41	119	[33]
	Slow	5.4×10^{-7}	- 150	64	[33]
$Rh_2(OH)^{3+}$	Fast	3.4×10^{-6}	140	146	[33]
	Slow	2.9×10^{-6}	-9	102	[33]
Cr_2^{4+}	Fast	3.6×10^{-4}	-40	81	[48]
	Slow	6.6×10^{-5}	0	97	[48]
$Cr_2(OH)^{3+}$	Fast	2.6×10^{-6}	174	157	[48]
	Slow	1×10^{-6}	23	114	[48]

[§]Complex names are abbreviated and explained in the text.

Table 3. Water-exchange rate parameters of trinuclear aqueous and acetate bridged clusters at 25°C.

Complex	k_{ex}^{298} (s^{-1}) ($^{c}H_2O$)	k_{ex}^{298} (s^{-1}) ($^{d}H_2O$)	$\Delta S^{\neq}$ (J $mol^{-1}K$)	$\Delta H^{\neq}$ (kJ mol^{-1})	Reference
$[Mo_3O_4(H_2O)_9]^{4+}$	1.5×10^{-3}	1.6×10^{2}	35[a]	71[a]	[52]
$[Mo_3S_4(H_2O)_9]^{4+}$	1.8×10^{-2}	7.5×10^{3}	107.6[a]	83[a]	[57]
Acetate bridged	k_{ex}^{298} (s^{-1})	$\Delta S^{\neq}$ (J $mol^{-1}K$)	$\Delta H^{\neq}$ (kJ mol^{-1})	$\Delta V_0^{\neq}$ (cm^3 mol^{-1})	Reference
$[Rh_3OAc_6(H_2O)_3]^{+}$	5×10^{-3}	43	99	5.3	[9]
$[Ru_3OAc_6(H_2O)_3]^{+}$	1.08×10^{-3}	85.1	116.9		[69]
$[Mo_3O_2Ac_6(H_2O)_3]^{2+}$	5.6×10^{-6}	77	126	8[b]	[68]
$[W_3O_2Ac_6(H_2O)_3]^{2+}$	1.02×10^{-6}	-164	58	-1.9[b]	[68]
$[W_3OAc_6(H_2O)_3]^{+}$	5.3×10^{-4}	-131	53		[68]

[a] data corresponds to $^{d}H_2O$

[b][8]

Table 4. Average bond lengths (Å) and angles for various Nb(V) and Ta(V) Lindqvist ions as measured using X-ray methods in the solid state.

Compound	M=O_t	μ_6-O-M[c]	[b]M-μ_2-O	M-μ_2-O-M[d]	Source
$[H_xNb_6O_{19}]^{(8-x)-(a)}$	1.793	2.366	1.990	114.3°	[95]
$Na_7[HNb_6O_{19}]\bullet 15H_2O$	1.770	2.379	1.994	114.5°	[94, 98]
$Na_8[Ta_6O_{19}]\bullet 15H_2O$	1.799	2.380	1.992	115.0°	[98]
$K_7Na[Nb_6O_{19}]\bullet 14H_2O$	1.796	2.364	1.993	114.0°	[94, 98]
$K_7Na[Ta_6O_{19}]\bullet 14H_2O$	1.813	2.365	1.986	114.6°	[115]
$Rb_8[Nb_6O_{19}]\bullet 14H_2O$	1.804	2.355	1.985	114.0°	[94]
$Rb_8[Ta_6O_{19}]\bullet 14H_2O$	1.817	2.358	1.979	114.7°	[94]
$Cs_8[Nb_6O_{19}]\bullet 14H_2O$	1.804	2.360	1.987	114.2°	[94]
$Cs_8[Ta_6O_{19}]\bullet 14H_2O$	1.811	2.353	1.975	115.2°	[116]

[a]($0 \leq x \leq 1$); [b]Excludes μ_2-OH-M bonds. [c]Error ±0.002 [d]Error ±0.1°.

Table 5. Rate parameters for exchange of water molecules from the inner-coordination sphere of Al(III) complexes to the bulk solution, as determined from ^{17}O-NMR

complex	k_{ex}^{298} (s^{-1})	$\Delta H^{\neq}$ (kJ mol^{-1})	$\Delta S^{\neq}$ (J $mol^{-1}K^{-1}$)	$\Delta V_0^{\neq}$ (cm^3 mol^{-1})	Reference
		monomeric complexes			
$[Al(H_2O)_6]^{+3}$	1.29	85	42	+5.7	[10]
$[Al(H_2O)_5OH]^{2+}$	3.1×10^4	36	-36		[117]
$[[AlF(H_2O)_5]^{2+}$	2.4×10^2	79	17		[118]
$AlF_2(H_2O)_4]^{+}$	1.6×10^5	65	53		[118]
$[Al(ssal)]^{+}$	3.0×10^3	37	-54		[119]
$[Al(sal)]^{+}$	4.9×10^4	35	-57		[119]
$[Al(mMal)]^{+}$	6.6×10^2	66	31		[120]
$[Al(mMal)]_2^{-}$	6.9×10^4	55	13		[120]
$[Al(ox)]^{+}$	1.1×10^2	69	25		[114]
		multimeric complexes			
ε-Al_{13}	1.1×10^3	53	-7		[121, 122]
$GaAl_{12}$	2.3×10^2	63	29	+3	[112]
$GeAl_{12}$	1.90×10^2	56	20		[123]
Al_{30}	rates are generally similar to those on the $GaAl_{12}$				[124]

abbreviations: ox=oxalate; ssal=sulfosalicylate; sal=salicylate; mMal=methylmalonate.

Table 6. Water-exchange rates and thermodynamic parameters of the ~2.5 nm sized $Mo_{72}Fe_{30}$ compared to the values for the $[Fe(H_2O)_6]^{3+}$ and various aminocarboxylate complexes at 25°C.

complex	k_{ex}^{298} (s^{-1})	$\Delta S^{\ddagger}$ (J $mol^{-1}K^{-1}$)	$\Delta H^{\ddagger}$ (kJ mol^{-1})	Reference
$Mo_{72}Fe_{30}$	6.7×10^6	-26	26.3	[5]
$[Fe(H_2O)_6]^{3+}$	1.6×10^2	12.1	64	[42]
$[FeEdta]^-$	6.8×10^7	-13	24.4	[125]
FeEdtaH	7.8×10^7	-20	22	[125]
$[FeCDTA]^-$	1.3×10^7	-25	25	[125]

FeEdta=Fe(III)-ethylenediaminetetraacetic acid; FeEdtaH= FeEdta with one acetic group protonated; FeCDTA=Fe(III) cyclohexanediaminetetraacetic acid.

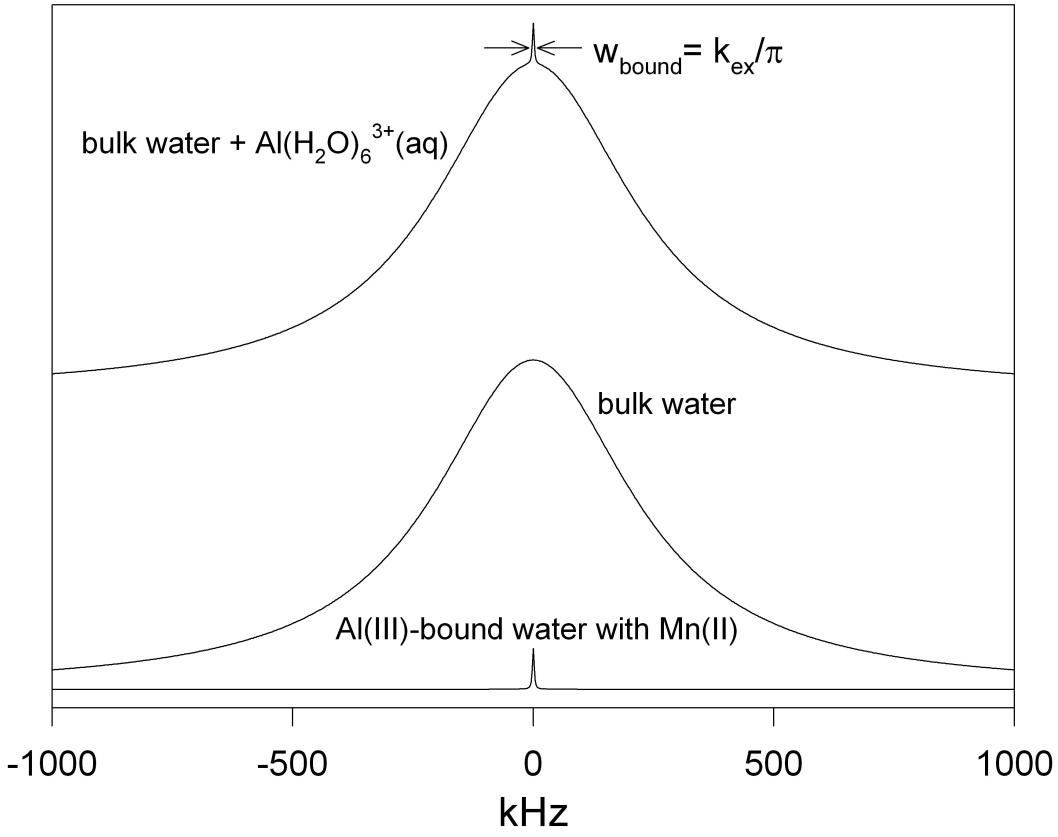

Figure 1. Addition of paramagnetic $Mn^{2+}_{(aq)}$ to a solution of a diamagnetic ion like $Al^{3+}_{(aq)}$ broadens the peak for the bulk water until it disappears into the baseline (bottom), leaving only the peak corresponding to the waters bound in the $Al^{3+}_{(aq)}$ complex.

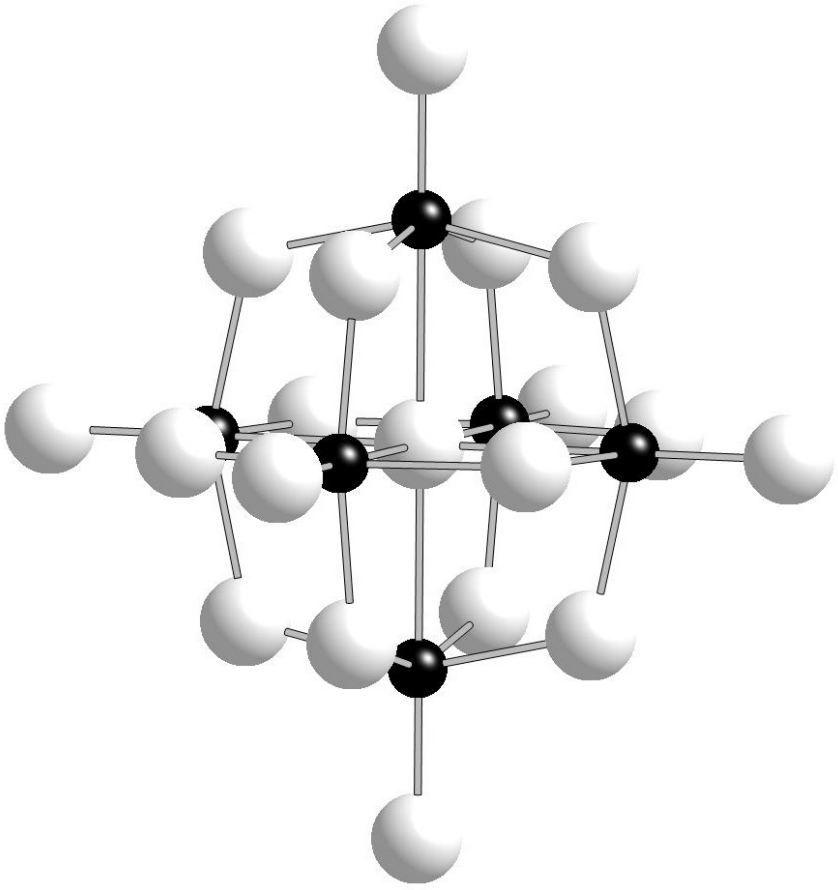

Figure 4. The Lindqvist ions, with the stoichiometry: $[H_xM_6O_{19}]^{(8-x)-}$ (M= either Ta(V) or Nb(V)) has a central μ_6-O sites that is inert to isotopic exchange, twelve μ_2-O bridges and six terminal η=O sites. In the ball-and-stick representation, the oxygens are light gray and the metals are black. Ions can also be synthesized with W(VI) and Mo(VI).

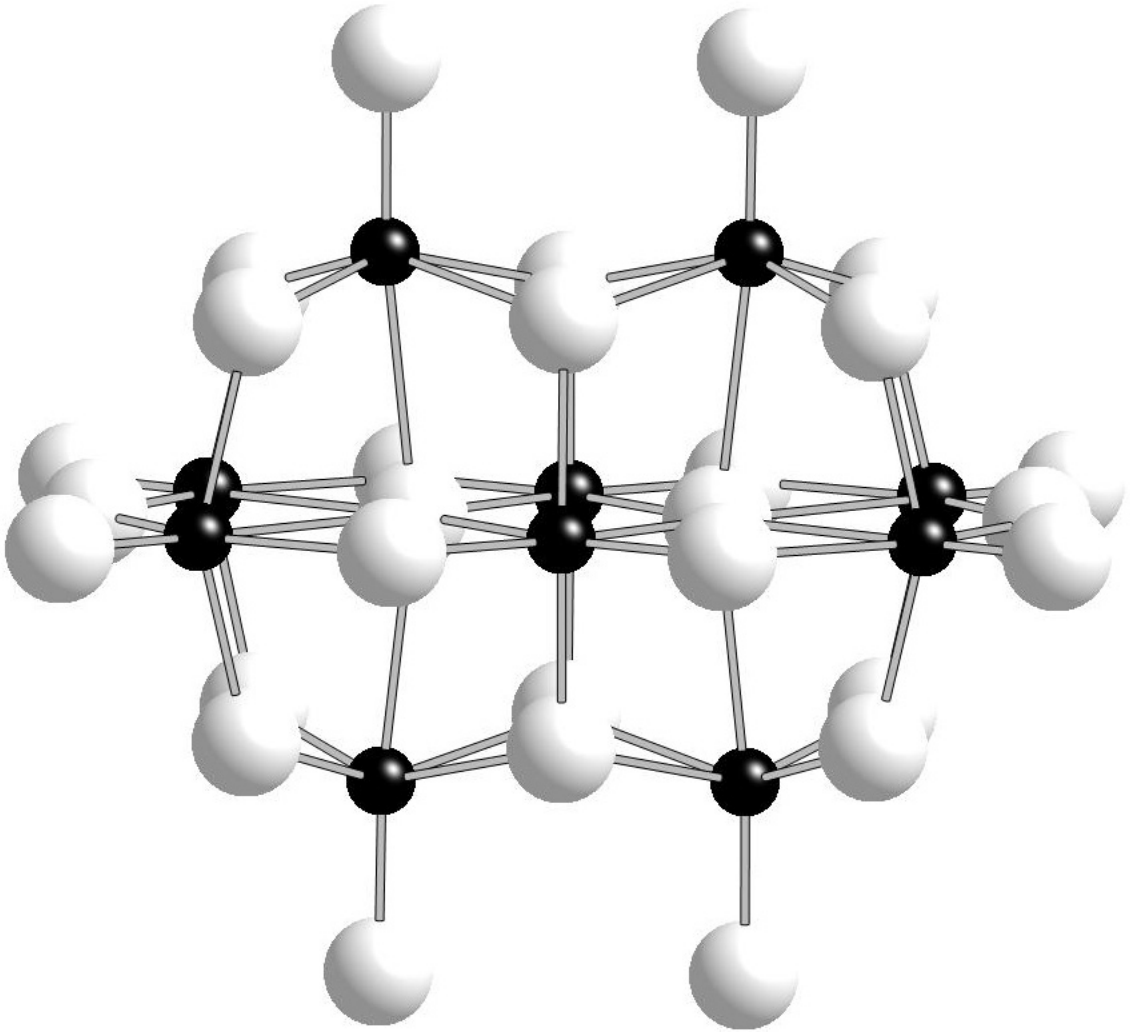

Figure 5. Structure of the decametallate ions having the stoichiometry: $[H_xM_{10}O_{28}]^{(6-x)-}$ where M=V(V), Nb(V) or Ta(V). In the ball-and-stick representation, the oxygens are light gray and the metals are black.

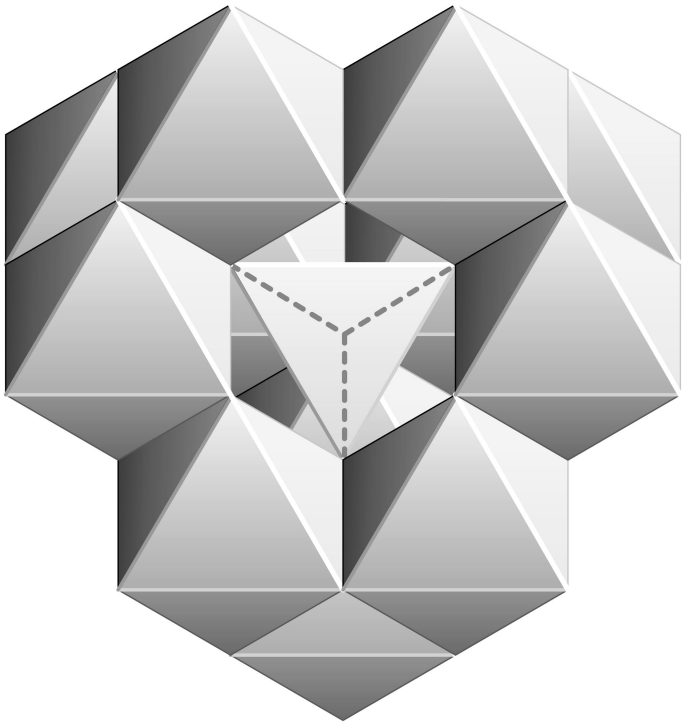

Figure 6. A polyhedral representation of the **MAl_{12}** ε-Keggin polyoxocations. These have the stoichiometry: $[MO_4Al_{12}(OH)_{24}(H_2O)_{12}]^{7/8+}$ with (M=Al(III), Ga(III), Ge(IV)). [111]. The octahedra correspond to $Al(O)_6$ and the tetrahedron corresponds to $M(O)_4$.

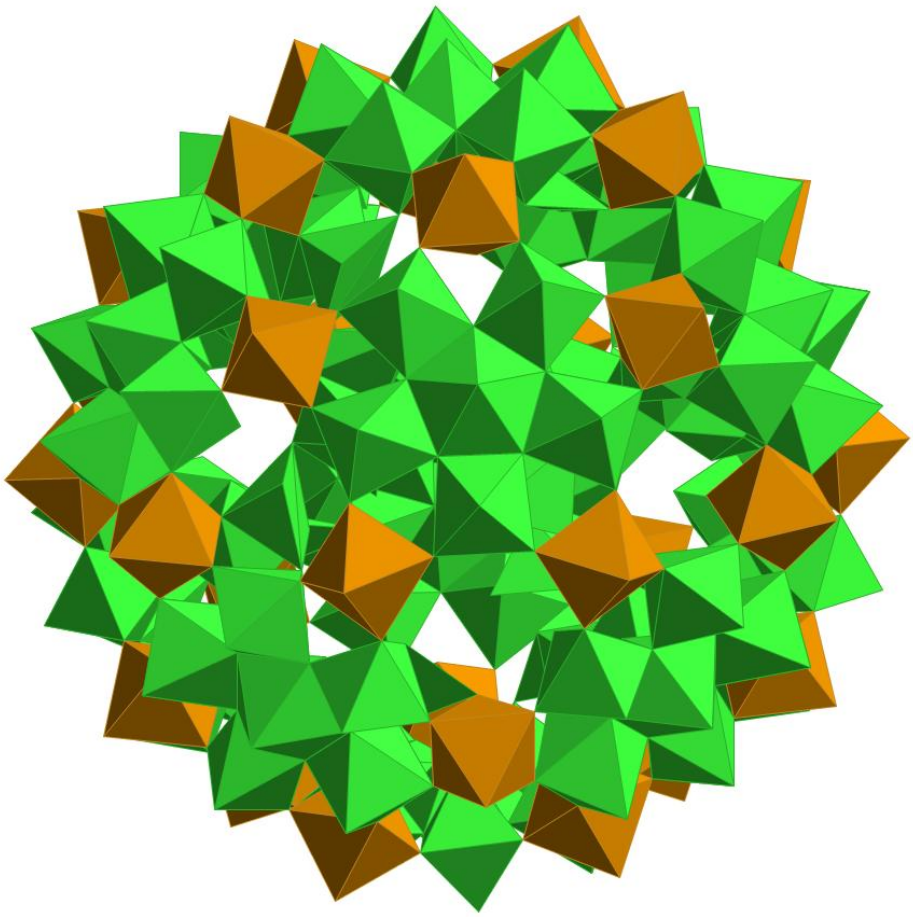

Figure 7. A near-spherical aqueous cluster, containing 72 Mo(VI)-oxide polyhedra (green) and 30 Fe(III) as $Fe(O)_6$ octahedra (brown).